Transport and Reaction Processes in Soil

Paul Sweeney (Problem presenter)   N Arab
Reza Bazarganzadeh   M Ceseri   Laura Gallimore
Andrew Lacey   Chris Lustri   Rooholah Majdodin
John Ockendon   Colin Please   Jean-Charles Seguis
Alex Shabala   Amy Smith   Nadia Smith   E Somfai
Robert Whittaker

ESGI 73, University of Warwick, April 2010

Contents

1 Introduction

Syngenta is one of the worlds leading agrochemical companies. In order to register agrochemicals in Europe it is necessary to have a detailed understanding of the processes in the environment that break down agrochemicals. The existing framework for environmental assessment includes a consideration of soil water movement and microbial breakdown of products in soil and these processes are relatively understood and represented in models. However the breakdown of agrochemicals by the action of light incident on the soil surface by a process termed photolysis is not so well represented in models of environmental fate. The problem brought by Syngenta to the workshop was how to include the effects of light degradation of chemicals into predictive models of environmental fate.

Photolysis is known to occur in a very thin layer at the surface of soil. The workshop was asked to consider how the very rough nature of the upper surface of a ploughed field might affect the degradation of chemicals by sunlight. The discussions were directed down two avenues: firstly to determine how the very small distances over which photolysis occurs might be adequately incorporated into models of transport in soils and, secondly to consider how the rough surface might modify the illumination of the surface and hence alter degradation.

The rate of degradation by photolysis is measured in the laboratory by illuminating a thin, typically about 1 or 2 mm, layer of soil with very strong xenon lamps. The amount of chemical is measured at various intervals and is fitted to a first-order process. Field experiments where the chemical is sprayed on a bare field show evidence of photolysis indicated by biphasic degradation patterns and the presence of breakdown products only formed by photolysis.

This report addresses methods for mathematically modelling the action of photolysis on particular relevant chemical species. We start with a general discussion of mechanisms that transport chemicals within soil §2. There is an existing computational model exploited by Syngenta for such modelling and we discuss how this performs and the predictions that can be derived using it §3.

The particular mechanism of photolysis is then considered. One aspect of this mechanism that is investigated is how the roughness of the surface of the soil could be adequately incorporated into the modelling. Some results relating to this are presented §4.2. Some of the original experimental data used to derive aspects of the model of photolysis are revisited and a simple model of the process presented and shown to fit the data very well §5. By considering photolysis with a constant diffusion coefficient various analytical results are derived and general behaviour of the system outlined. This simple model is then applied to real field-based data and shown to give very good fit when simply extended to account for the moisture variations by utilising moisture dependent diffusion coefficients derived from the existing computational model §5.3. Some consequences of the simple model are then discussed §6.

2 Transport mechanisms in soil

There was considerable discussion at the workshop on what mechanisms should be accounted for when considering transport of chemical species in soil. Many of these are included in the existing computational model PEARL [4] used by Syngenta, but here we briefly consider some of these.

The first aspect of the model is to consider how the moisture content of soil varies. The subject of water flow in soil is a very well established subject with a huge literature (see for example [1, 2]). In using these ideas we must account for gravity acting to draw the water down while capillary effects within the solid porous structure created by the soil holds the water up. When considering the aspects of soil relevant here we need also to add to this the processes of additional water entering the system primarily through the upper surface as rain and also the removal of water due to evaporation. Such evaporation may, in the simplest form, be taken to be water flux from the upper surface but in more detail it may be necessary to consider vapour movement through the depth of the soil out into the atmosphere. Note that models of water flow in soil separate the soil into two different types of behaviour, saturated and unsaturated depending on whether the water fills the pores or not. In the circumstances of interest here the upper region of the soil is unsaturated. Hence models exist, usually based on Richards equation and extensions thereof that determine the degree of saturation and the water flow velocity through the depth of the soil as a function of time.

The various chemical species applied to the soil are usually considered to be in such small quantities that they have insignificant effect on the flow and distribution of water in the soil. The one exception to this separation of mechanisms is probably when surfactants are applied which may significantly alter the surface tension, and hence the capillary effects, even for very low concentrations. Here we shall not consider such interactions. The species are transported by the water due to advection and diffusion in the water. It is usually assumed that the macroscopic behaviour for the interaction between water flow and diffusion within a highly tortuous porous media can be accounted for by introducing the concept of dispersion. This approach seems appropriate in these circumstances.

One significant complication to consider when representing movement of chemicals through soil is that the species may exit in some bound state on the soil particle surface and in some other state within the water. Such behaviour is typically represented by considering reaction between the two states and in practice these reactions are taken to be so quick that there is simply a partition coefficient between the stationary species attached to the soil and the species within the adjacent fluid.

As the chemical moves through the soil is can be broken down into other species by a variety of mechanisms and reactions. These reactions depend on the local concentrations of the relevant species but may be further regulated by other species such as the local pH. Of these reactions those commonly considered are oxidation, microbial degradation and photolysis. Here we shall not consider oxidation and briefly consider microbial action, which we shall take to be at a constant rate, although in practice this rate is strongly dependent on the local moisture content through mechanisms such as altering the microbial population.

Our main interest will be with photolysis where the chemicals species are broken down by UV radiation from the sun.

Photolysis depends on UV radiation encountering the chemical species and degrading it into other species. One aspect of the modelling is to determine how much radiation penetrates into the surface of the soil. This will depend not only on the local structure of the soil but also on the overall surface topography. One approach to modelling such behaviour is to consider what the "effective area" of the surface when projected down onto a planar surface and whether this effective area is different from the actual projected area. We shall consider this question in §4.2. When UV radiation encounters the chemical species there can be direct photolysis, where the chemical is immediately degraded, or there can be indirect photolysis where the UV ionises radials of various sorts and these are transported to a place where they subsequently react with the chemical species to degrade it. It is believed that for the chemicals of interest here only direct photolysis is important so the indirect methods were not considered.

3   Current chemical transport model

PEARL [4] is a model commonly used to model the movement of chemicals through soil. This model has a huge number of options but for the purposes here we restricted our attention to those aspects related to transport in a soil without any plants. The model uses the Richards equation to describe the motion of the moisture accounting for variations in viscosity and capillary strength. The transport of each of the possible chemical species is then considered allowing for advection, diffusion and dispersion as well as chemical reactions. The reactions are described by rates that may vary both in time and in position. This variation may be due differing soil types, due to moisture content variations changing the microbe behaviour, or due to proximity of the upper soil surface such as occurs with photolysis.

The details of the numerical method used to solve the problem are not completely clear as the source code is not available. However, there appears to be the concept of solution nodes being the centrepoint of "layers" in the model. Timestepping within the model appears to be constrained so that the solution is stable but the accuracy of the method appears not to be discussed. In most simulations done by Syngenta, a minimum "layer" size of 2mm is used. If behaviour is expected on a lengthscale of this size or shorter then numerical diffusion may swamp behaviour of the solution (Appendix 1 gives a brief outline of of this process).

An example output from the model used by Syngenta and its comparison with field data is shown in figure 1. This field data shows rapid reduction in chemical concentration in first 5 to 10 days, followed by a much slower decay. The initial decay is presumed to be due to the rapid process of photolysis while the longer behaviour is identified as being due to the slower microbe action. Although the model can be parameterised to represent both processes, in practice this is rarely done as it is often assumed that microbial degradation is the dominant process. The workshop considered that the lack of any predicted fast
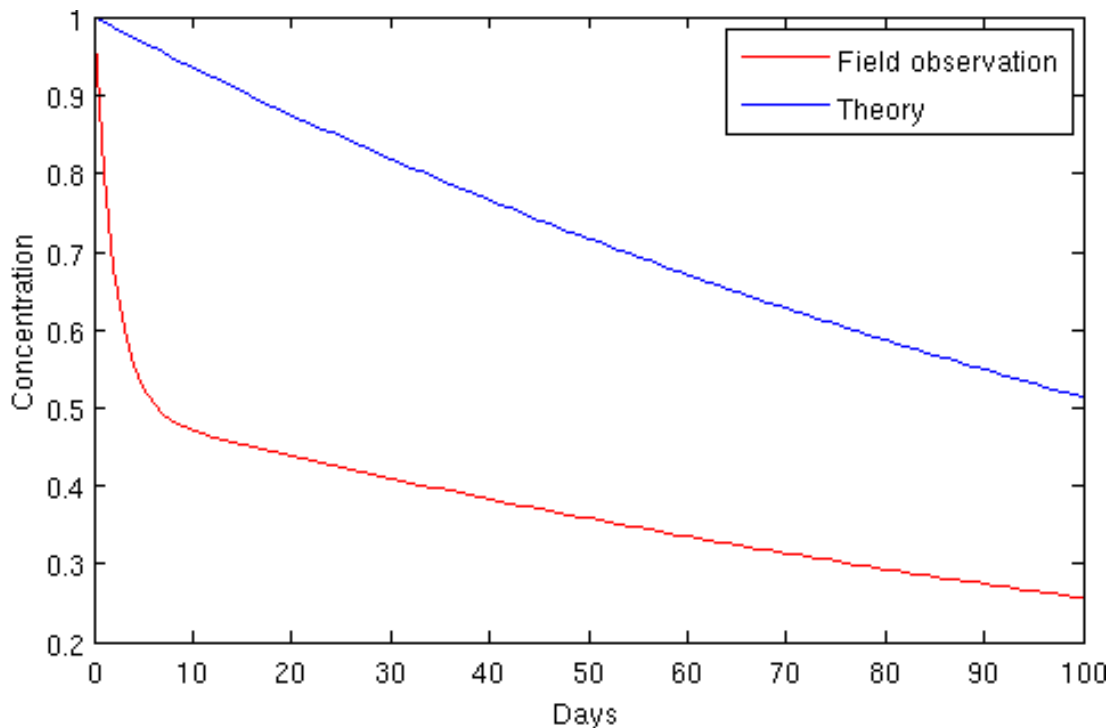
Figure 1: A comparison of field data from a Syngenta trial with the theoretical prediction using the PEARL [4] package. Non-dimensional concentration of chemical in the top 30cm of soil is plotted as a function of time.

behaviour by the model may be due to excessive numerical diffusion swamping the rapid photolysis that only occurs in a narrow surface at the top of the soil.

4 Photolysis

4.1 The photolytic effect

We now consider the process of photolysis of chemicals in soil. This problem has been studied by a numerous of authors. The work by Hebert etal. [5] is the first substantial paper on the topic of photolysis in soils looking at degradation rates in various thickness of different soils.. In the work by Konstantinou etal. [6] does further work but includes comparisons of degradation when there is no sunlight to quantify the effects of microbial decay. The paper presented a substantial amount of data from experiments along with functional forms used for fitting these. In Ciani etal [7] a model is developed of light reflection, absorption and transmission through a thin soil sample and this is compared to experimental data. The resulting fits indicate that the simple concept of an absorption depth as function of wavelength is a good model for the behaviour. They also indicate that the absorption can depend on the moisture, although we have not considered this. In
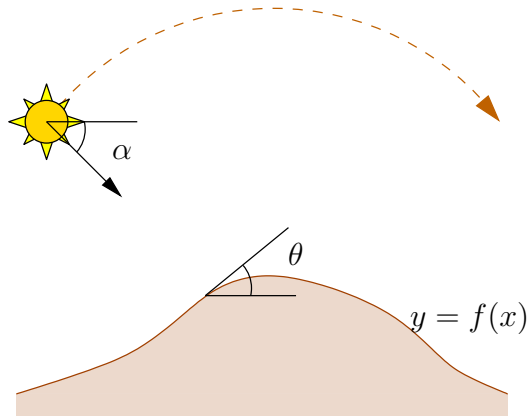
Figure 2: A sketch showing the sun illuminating a non-planar solid surface $y = f(x)$, defining the co-zenith angle α and the slop angle θ of the soil. The latter satisfies $\tan\theta = y'(x)$.

Frank etal. [8] various chemical on soils are considered and there is particularly interesting data on the degradation in different depths of soil and moisture.

Most of the degradation of the chemical occurs at wavelengths around $\nu = 300$nm (this is in the UV spectrum). At these wavelengths the typical penetration length of this radiation into soil is very small being 0.2–0.3mm. Such measurements have been made using thin layers of soil and determining the strength of the transmitted light through the sample.

4.2 Modelling the intensity of light through the soil

In order to determine the effect of shadowing on the soil, we determined the intensity received by a given point on a field at time t using elementary methods. We first consider a field that varies in only the x-direction such that the surface of the field is described as $y = f(x)$. The angle between the sun and the ground given by $\alpha(t)$. A schematic of this configuration may be seen in Figure 2.

Assuming that the intensity of the Sun is given by I_S, which is typically found to be approximately 1000 W/m^2, we find that the intensity at x for time t, denoted $I(x,t)$, is given by

$$I(x,t) = I_S \max\left\{0, \frac{f'(x)\cos(\alpha(t)) + \sin(\alpha(t))}{\sqrt{1 + f'(x)^2}}\right\}. \tag{1}$$

The use of the maximum expression ensures that the amount of intensity received at a particular point does not decrease below zero. If the intensity is equal to zero, the point is assumed to be in shadow. Now, this does not capture all possible shadowing behaviour as it does not consider the rays of light being blocked by nonlocal obstructions. To allow for nonlocal obstructions would require a more complicated application of ray theory which was not considered here.

6
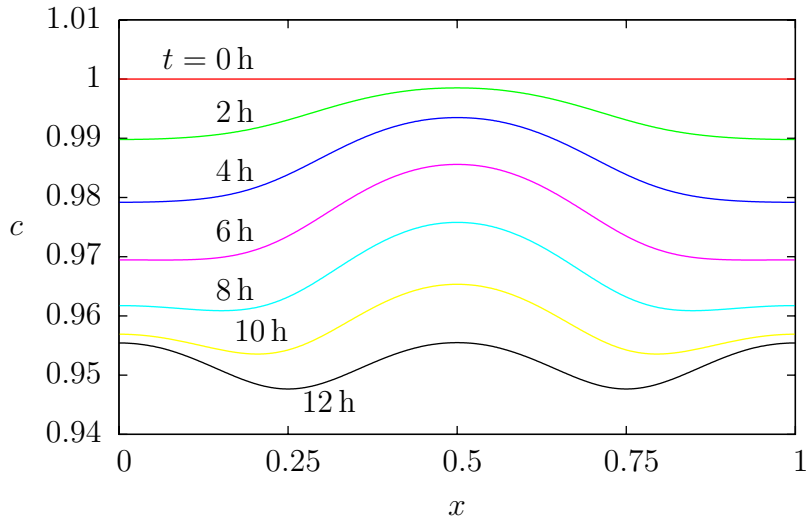
Figure 3: Degradation of chemical present in an undulating field over the span of one day. The non-dimensional concentration c is plotted as a function of horizontal position x at various values of time t.

It is reasonable to assume that the degradation of chemical in soil by sunlight is proportional to the intensity of the light and concentration of chemical present at that location. Therefore, we have

$$\frac{\partial C}{\partial t} \propto I\,C\,, \tag{2}$$

where C is the concentration of chemical present at a particular location in the field. We may use the expression obtained for the intensity of light at a point in the field, $I(x,t)$, to produce

$$\frac{\partial C}{\partial t} = -kI_S \max\left\{0, \frac{f'(x)\cos(\alpha(t)) - \sin(\alpha(t))}{\sqrt{1 + f'(x)^2}}\right\} C\,, \tag{3}$$

where k is a constant of proportionality. Experimental data provided by Syngenta indicated that the chemical has a half-life of around 5 days under full intensity, or $kI_s \approx 0.13$/day. Finally, we investigated the chemical breakdown on an example field over the course of one day by applying it to a test scenario. An example field was given with a surface height of $y = 0.1\sin(2\pi x)$ over one unit of length, with the angle of the sun, $\alpha(t)$, varying from $\pi/6$ to $5\pi/6$ over the course of a twelve hours or one half day, according to the linear equation

$$\alpha(t) = \pi/6 + 4t\pi/3, \qquad 0 \le t \le 1/2 \text{ days}\,. \tag{4}$$

The degradation of the chemical, and therefore the resultant change of chemical concentration, may be seen in Figure 3.

We see that the degradation is nonuniform and hence if the initial distribution of chemical on the surface is uniform then it will become nonuniform. The points which face
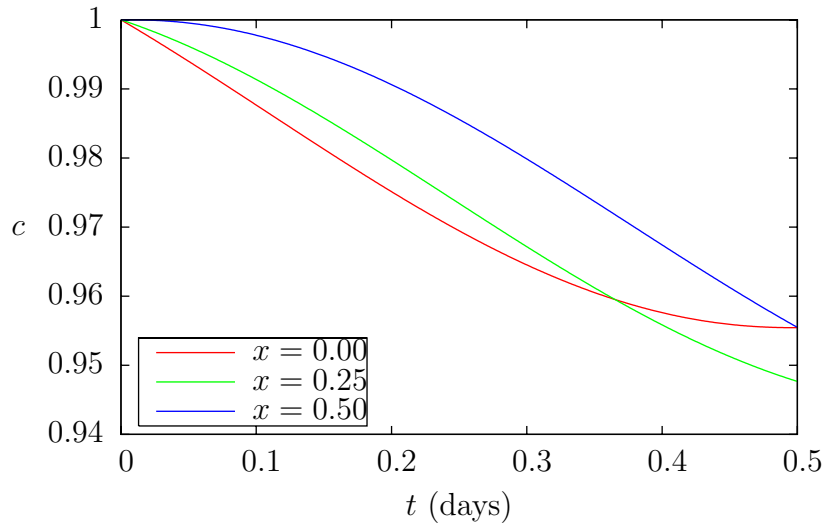
Figure 4: Degradation of chemical present in an undulating field over the span of one day. The non-dimensional concentration c is plotted as a function of time t at three different horizontal locations x.

the sun in the morning degrade quickly, but then degrade more slowly in the afternoon, while points which face the sun in the afternoon degrade more quickly in the afternoon than in the morning. The behaviour at three such points on the sinusoidal surface are shown in figure 4. Comparing these results to those of a flat field ($y = 0$), which may be seen in figure 5, that has been presented in this manner to compare with figure 3, and shows that more chemical is degraded on a flat surface than on a varying surface due to shadowing effects. Therefore, shadowing appears to play a significant role that should be taken into account if there is some variation on the surface of the field.

4.3   Fractal Nature of Soil

Fractal approaches may be applied to systems that demonstrate a level of self-similarity on multiple size-scales. Such modelling approaches are convenient in that they describe this multiscale structure using a single parameter, known as the fractal dimension D. In practice this self-similarity does not extend infinitely, and as such there are limitations on the range of scales in which these techniques may be applied.

In the context of soil, we find that there is a level of structure that takes place on the scale of pores, as well as the overall structure of the field. This indicates that a fractal may be applied in order to describe the structure of the soil region. A number of formulations have been presented for fractal interpretations of soil [9, 10]. It should be noted, however, that such behaviour only extends down to the scale of pores and up to a maximum scale. Outside this range, the interpretations is no longer valid. For the problems of interest here, both for deposition of the chemical and illumination by the sun the quantity of interest is the effective surface area of the field when view on a scale much bigger than a pore. We
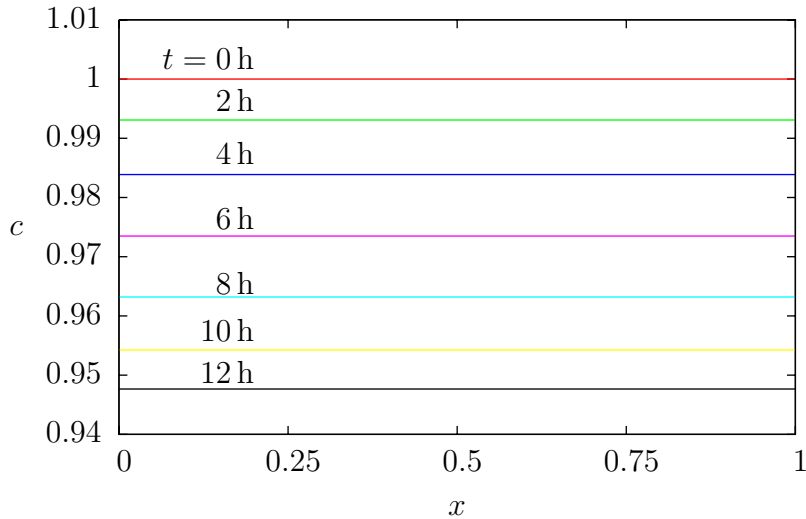
Figure 5: Degradation of chemical present in a flat field over the span of one day. The non-dimensional concentration c is plotted as a function of horizontal position x at various values of time t.

consider what is surface area is in terms of the projected surface area of the field.

An expression for the surface fractal dimension of a porous medium was developed [9], and given as

$$D = 2 + 3\frac{\phi^{4/3} + (1 - \phi)^{2/3} - 1}{2\phi^{4/3}\ln(\phi^{-1}) + (1 - \phi)^{2/3}\ln((1 - \phi)^{-1})} ,$$ (5)

where ϕ is the porosity of the porous medium, in this case the soil. Typical values for D fall within the range $2 \leq D \leq 2.2$ [9]. In order to find the effective surface area using the fractal dimension, we determine the ratio between the original measuring scale and the pore scale, or the effective area ratio. This ratio may be calculated as

$$A_{rat} = \left(\frac{L_{max}}{L_{min}}\right)^{D-2} ,$$ (6)

where D is the fractal dimension of the surface, L_{min} is the minimum length scale of interest, or the size of the pores, and L_{max} is the maximum length scale of interest, which does not appear to have been determined. This seems like it would be the scale of the largest pore-like variation within the field, or the largest 'soil clumps' that may be found in the area of interest. As such, if the original field had area A, the effective surface area on a pore scale would be $A_{rat}A$. Using typical values, such as $L_{max} = 20$mm, $L_{min} = 0.1$mm and $D = 2.2$mm, this gives an effective surface area ratio of 2.8.

This analysis indicates that the effective surface area is much larger than the projected surface area due to the multiscale structure of soil If we now wish to incorporate these ideas into our previous modelling of degradation of the chemical it is not straightforward. Two fundamental issues arise. Firstly it is necessary to determine how the chemical is

9

deposited onto the fractal surface when it is applied, at a uniform rate over the projected surface are of the field by the spraying equipment. Secondly we must determine how the fractal behaviour should be accounted for in the previous analysis of illumination onto an uneven surface. We have already identified that such unevenness reduces the effective of the illumination relative to a flat surface. Hence such a decrease must be incorporated into any effective illumination strength on the surface.

We have not pursued this avenue of investigation further but believe that these effects might be incorporated into the model developed in §4.2, perhaps changing (2) such that it becomes

$$\frac{\partial C}{\partial t} \propto A_{eff} I \, C \; , \tag{7}$$

where A_{eff} would depend both on the A_{rat} and the effective illumination of the surface.

5 Simple transport models of photolysis degradation

Because photolysis occurs in a very thin layer a model that concentrated on behaviour in this thin layer was developed during the workshop. The aim was to exploit the existing models to determine the moisture distribution and movement within the soil and to use this to characterise the chemical transport in a very thin planar surface layer of the soil. Such modelling should identify the critical parameters and their interactions. The modelling also returned to the original experimental data in order to determine more accurately the parameters within the model of photolysis.

5.1 Photolytic degradation with no transport

5.1.1 Laboratory experiments

Laboratory experiments performed by Syngenta involve a thin layer of well-mixed dry soil initially containing a mass M_0 of chemical. The layer is then illuminated from above by a light of specified intensity, and the mass of chemical, $M(t)$, remaining is recorded at regular time intervals. The layer depth h is typically 1–2 mm, and the light intensity I_0 a few times greater than the average light intensity in natural conditions. See figure 6.

5.1.2 Modelling

We construct a simple one-dimensional model for photolytic degradation in a layer of depth h and horizontal area A. We assume that light intensity $I(x)$ falls off exponentially with distance x into the layer, and that the degradation rate D per unit mass of soil is proportional to the concentration C of chemical and to the light intensity. We introduce the surface intensity I_0, a solar decay constant α, and a reaction rate k, and write

$$I(x) = I_0 e^{-\alpha x} \, , \qquad D = kCI \, . \tag{8a,b}$$
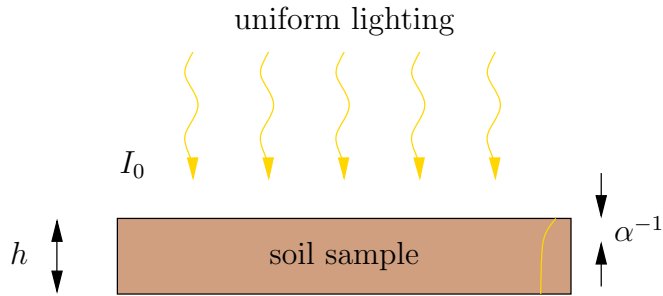
Figure 6: A sketch of the experimental setup described in §5.1.1, showing uniform illumination of a soil layer of depth h. The initial light intensity is I_0, and the solar penetration depth is α^{-1}.

We shall refer to the quantity $1/\alpha$ as the solar penetration depth. We also assume that the mass M_0 of chemical starts off uniformly distributed throughout the layer, that there is no diffusive or advective transport. Hence

$$\frac{\partial C}{\partial t} = -D, \qquad C = \frac{M_0}{Ah} \quad \text{at} \quad t = 0. \tag{9a,b}$$

Combining equations (8) and (9), we arrive at the following model for the concentration $C(x,t)$:

$$\frac{\partial C}{\partial t} = -kI_0 e^{-\alpha x} C, \tag{10}$$

subject to an initial condition $C(x,0) = M_0/(Ah)$. The mass M of chemical remaining at time t is given by

$$M(t) = A \int_0^h C(x,t)\, dx. \tag{11}$$

5.1.3 Solution

We non-dimensionalise the variables in the obvious way by writing

$$C = \frac{M_0}{Ah} c, \qquad x = h\xi, \qquad t = \frac{\tau}{kI_0}, \qquad M = M_0 \mu. \tag{12a–d}$$

Using these in the model (10) gives

$$\frac{\partial c}{\partial \tau} = -e^{-\chi \xi} c, \quad \text{subject to} \quad c(\xi,0) = 1, \tag{13a,b}$$

where $\chi = \alpha h$ is a non-dimensional layer depth. From (11) the fraction of chemical remaining is given by

$$\mu(\tau) = \int_0^1 c(\xi,\tau)\, d\xi. \tag{14}$$

11
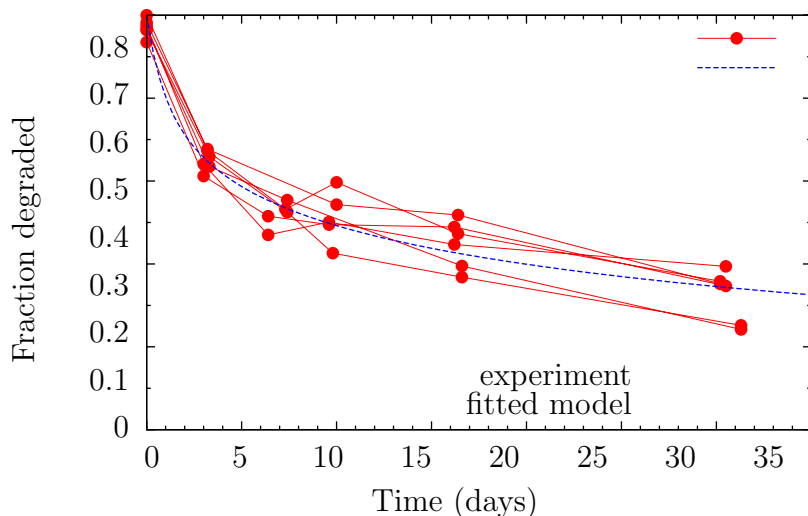
Figure 7: Experimental data from Syngenta for the experiment described in §5.1.1, with $h = 1\,\mathrm{mm}$. Also shown is the theoretical prediction (18) with parameters $I_0 k = 2.3\,\mathrm{day}^{-1}$ and $\alpha = 7.3\,\mathrm{mm}^{-1}$ chosen using a least-squares fit to the data.

The solution to (13) is

$$c(\xi, \tau) = \exp(-e^{-\chi\xi}\tau). \tag{15}$$

Substituting this into (14) and using the substitution $u = \tau e^{-\chi\xi}$, we obtain

$$\mu(\tau) = \int_{\tau e^{-\chi}}^{\tau} \frac{\mathrm{e}^{-u}}{u}\,\mathrm{d}u = \mathrm{E}_1(\tau e^{-\chi}) - \mathrm{E}_1(\tau). \tag{16}$$

where

$$\mathrm{E}_1(z) = \int_z^\infty \frac{\mathrm{e}^{-t}}{t}\,\mathrm{d}t \tag{17}$$

is an exponential integral.

Rewriting (16) back in the dimensional variables, we have that

$$M(t) = \frac{M_0}{\alpha h}\Big(\mathrm{E}_1(I_0 kt e^{-\alpha h}) - \mathrm{E}_1(I_0 kt)\Big). \tag{18}$$

5.1.4   Comparison with experimental data

Some data was available from laboratory experiments carried out by Syngenta, which showed the fraction M/M_0 of chemical remaining at various times, for six repetitions of the same experiment. This data is plotted in figure 7.

We note that the decay curves are far from exponential. In particular observe that the time taken for the the level to drop to 50% is much shorter than the time to drop from 50% to 25%. Hence we conclude that attempts to fit data in figure 7 with an exponential will give poor reproduction of the behaviour.

12

Also shown in figure 7 is a curve found by fitting the simple model solution (18) to the data in a least-square sense by choosing parameter values for α and for $I_0 k$. The values determined in this manner are

$$I_0 k = 2.3 \, \text{day}^{-1} \qquad \alpha = 7.3 \, \text{mm}^{-1} \tag{19}$$

This simple model gives predictions that are able to fit the data very well. This new model appears to better explain the data from the laboratory experiments than previous work. However, there is a need to examine this model more carefully as fitted values of the two parameters kI_0 and α may not be physically reasonable. In particular α indicates that the decay distance for UV in soil is $1/7.3 \approx 0.14$mm and this would appear to be significantly smaller that the value measured by other means. We have yet to completely reconcile this aspect of the work.

5.2 Photolytic degradation with constant diffusion

We will discuss in more detail extensions to the modelling to account for realistic field conditions in §5.3 However, it is very instructive to consider the slightly more realistic model of a chemical that is applied to the surface of an infinitely deep soil layer, and can spread downwards by diffusion, as well as being degraded by the sunlight. Equation (10) is modified by a diffusion term to become

$$\frac{\partial C}{\partial t} = D_{\text{e}} \frac{\partial^2 C}{\partial x^2} - kI_0 e^{-\alpha x} C \,, \tag{20}$$

for $0 < x < \infty$, where D_{e} is the constant effective diffusivity. The initial and boundary conditions are given by

$$C = \frac{2M_0}{A} \delta(x) \quad \text{at} \quad t = 0 \,, \tag{21a}$$

$$\frac{\partial C}{\partial x} = 0 \quad \text{at} \quad x = 0 \,, \qquad C \to 0 \quad \text{as} \quad x \to \infty \,. \tag{21b,c}$$

The introduction of an effective diffusion coefficient D_{e} means that, if we were to apply (13), there would then be a dimensionless parameter in the system, which we can write as a Damköhler number:

$$Da = \frac{I_o k}{\alpha^2 D_{\text{e}}} \tag{22}$$

This gives the ratio of the typical diffusion time over the solar penetration depth α^{-1}, to the degradation time scale $(I_0 k)^{-1}$.

In physical situations D_{e} is not constant but depends very strongly on the moisture content of the soil as is discussed in §5.3. Hence in order to understand the general behaviour it is therefore instructive to consider the two limiting cases of $Da \gg 1$ or $Da \ll 1$.
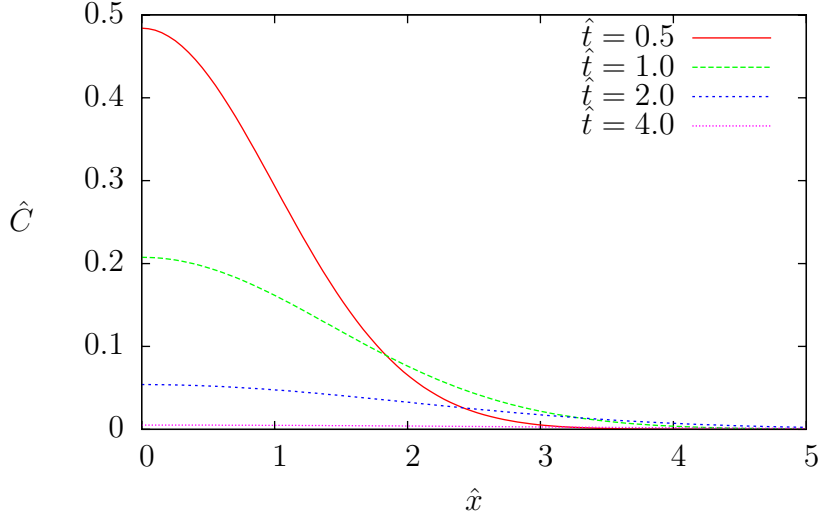
Figure 8: Vertical concentration profiles for the large-Da asymptotic solution (27b), using the non-dimensionalisation (23).

5.2.1 Asymptotics for large Damköhler number ($Da \gg 1$)

If $Da \gg 1$, then the chemical will be degraded before it has had the chance to diffuse over the solar penetration depth. The relevant time scale is thus the degradation time $T \sim (I_0 k)^{-1}$ and the relevant length scale is the distance $L \sim (D_e T)^{1/2}$ over which the chemical can diffuse in that time. The typical concentration level is set by $M_0/(AL)$. We therefore non-dimensionalise the variables as

$$x = \left(\frac{D_e}{I_0 k}\right)^{1/2} \hat{x}, \qquad t = \frac{1}{I_0 k}\hat{t}, \qquad C = \frac{M_0}{A}\left(\frac{I_0 k}{D_e}\right)^{1/2} \hat{C}, \qquad (23\text{a–c})$$

and arrive at the following system:

$$\frac{\partial \hat{C}}{\partial \hat{t}} = \frac{\partial^2 \hat{C}}{\partial \hat{x}^2} - e^{-\hat{x}/Da}\hat{C}, \qquad (24\text{a})$$

subject to

$$\hat{C} = 2\delta(\hat{x}) \quad \text{at} \quad t = 0, \qquad \frac{\partial \hat{C}}{\partial \hat{x}} = 0 \quad \text{at} \quad x = 0, \qquad \hat{C} \to 0 \quad \text{as} \quad \hat{x} \to \infty. \qquad (24\text{b–d})$$

For $Da \ll 1$ the exponential in (24a) is close to unity, over the range of $\hat{x}$ where $\hat{C}$ is appreciable. Making this approximation, and writing $\hat{C}$ as

$$\hat{C} = \breve{C}(\hat{x}, \hat{t})\, e^{-\hat{t}}, \qquad (25)$$

equation (24) becomes

$$\frac{\partial \breve{C}}{\partial \hat{t}} = \frac{\partial^2 \breve{C}}{\partial \hat{x}^2}, \qquad (26)$$

14

subject to the same initial and boundary conditions as (24). This is now a standard diffusion problem, with a similarity solution given by

$$\check{C}(\hat{x}, \hat{t}) = \frac{1}{\sqrt{\pi \hat{t}}} e^{-\hat{x}^2/(4\hat{t})} \qquad \Rightarrow \qquad \hat{C}(\hat{x}, \hat{t}) = \frac{1}{\sqrt{\pi \hat{t}}} e^{-\hat{t}} e^{-\hat{x}^2/(4\hat{t})} \,. \tag{27a,b}$$

Returning to dimensional variables we have

$$C(x, t) = \frac{M_0}{A} \left(\frac{I_0 k}{D_e} \right)^{1/2} e^{-I_0 k t} e^{-x^2/(4 D_e t)} \,. \tag{28}$$

We can interpret the solutions as indicating that if diffusion is very small then the chemical does not move far and remains confined to a layer much smaller that the solar penetration depth. Hence the chemical undergoes essentially uniform solar degradation. Concentration profiles at various times are shown in figure 8.

5.2.2 Asymptotics for small Damköhler number ($Da \ll 1$)

If $Da \ll 1$ then the chemical will spread much deeper than the solar penetration depth before significant degradation has taken place. The rapid diffusion will mean that the concentration is almost uniform over the solar penetration depth at the surface. There will therefore be two regions to consider: an inner region near the surface of depth α^{-1} where photolytic degradation occurs, and an outer region of depth $L \gg \alpha^{-1}$ dominated by the diffusive spreading. Both regions will have the same time and concentration scales, but the length L has yet to be determined.

To spread over a length scale L by diffusion will take a time $T \sim L^2/D_e$. Once spread over this length, the chemical will have typical concentrations of $O(M_0/(AL))$. However, the degradation takes place only over the initial $O(\alpha^{-1})$ depth, so the time to have a significant amount of M_0 degrade is lengthened from the previous estimate by a factor of αL. The relevant time scale for the degradation is therefore $T \sim \alpha L/(I_0 k)$. Equating the two time scales, we find $L \sim \alpha D_e/(I_0 k)$ and $T \sim \alpha^2 D_e/(I_0 K)^2$. We therefore adopt the scalings

$$x = \frac{1}{\alpha} \bar{x}, \qquad t = \frac{\alpha^2 D_e}{(I_0 K)^2} \bar{t}, \qquad C = \frac{M_0 I_0 k}{A D_e} \bar{C}, \tag{29a–c}$$

for the inner region, and

$$x = \frac{D_e}{I_0 k} \tilde{x}, \qquad t = \frac{\alpha^2 D_e}{(I_0 K)^2} \tilde{t}, \qquad C = \frac{M_0 I_0 k}{A D_e} \tilde{C}, \tag{30a–c}$$

for the outer region.

In the inner region, the system (24) becomes

$$Da^2 \frac{\partial \bar{C}}{\partial \bar{t}} = \frac{\partial^2 \bar{C}}{\partial \bar{x}^2} - Da \, e^{-\bar{x}} \, \bar{C} \,, \tag{31a}$$

15
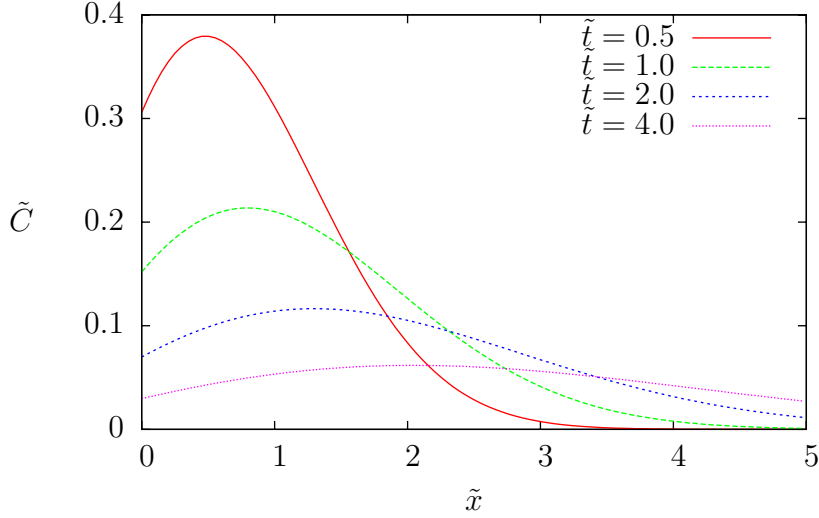
Figure 9: Numerically computed vertical concentration profiles for the outer layer of the small-Da asymptotic system (34) and (38), using the non-dimensionalisation (30).

subject to

$$\frac{\partial \bar{C}}{\partial \bar{x}} = 0 \quad \text{at} \quad \bar{x} = 0 \,. \tag{31b}$$

There will also be a matching condition with the outer layer as $\bar{x} \to \infty$, and an initial condition, both of which we shall consider later.

Solving (31) as a power series in Da, we find that

$$\bar{C}(\bar{x}, \bar{t}) = \bar{C}_0(\bar{t}) + Da\left(\bar{C}_1(\bar{t}) + \bar{C}_0(t)\,(\bar{x} + e^{-\bar{x}})\right) + O(Da^2) \,, \tag{32}$$

where $\bar{C}_0(\bar{t})$ and $\bar{C}_1(\bar{t})$ are (at this stage) unknown functions of $\bar{t}$.

In the outer region, the system (24) becomes

$$\frac{\partial \tilde{C}}{\partial \tilde{t}} = \frac{\partial^2 \tilde{C}}{\partial \tilde{x}^2} - \frac{1}{Da} e^{-\tilde{x}/Da}\, \tilde{C} \,, \tag{33a}$$

subject to

$$\tilde{C} \to 0 \quad \text{as} \quad \tilde{x} \to \infty \,, \tag{33b,c}$$

and the matching condition

$$\tilde{C} \sim \bar{C} \quad \text{as} \quad \tilde{x} \to 0 \ \& \ \bar{x} \to \infty \,. \tag{33d,e}$$

Again there will also be an initial condition, which we shall consider later.

At $O(Da^n)$ for any $n \in \mathbb{Z}_0^+$, the governing equation (33a) simplifies to

$$\frac{\partial \tilde{C}}{\partial \tilde{t}} = \frac{\partial^2 \tilde{C}}{\partial \tilde{x}^2} \,. \tag{34a}$$

16

Using the expression (32) for $\bar{C}$, the matching condition (33d) becomes $\tilde{C} \sim \bar{C}_0(t)(1 + \tilde{x})$ as $\tilde{x} \to 0$ at leading order. This implies that the appropriate boundary conditions on $\tilde{C}$ in the outer region can be rewritten from (33a) to be

$$\frac{\partial \tilde{C}}{\partial \tilde{x}} - \tilde{C} = 0 \quad \text{at} \quad \tilde{x} = 0 , \qquad \tilde{C} \to 0 \quad \text{as} \quad \tilde{x} \to \infty . \tag{34b,c}$$

We therefore have a standard diffusion problem with a Robin (mixed) boundary condition at $x = 0$, which encapsulates the effect of the photolysis layer.

Finally, in order to determine the initial condition for (34), we must examine the behaviour of the system at smaller times. The above two-region solution assumes that the diffusive spreading has caused the chemical to spread much deeper than the solar penetration depth. The relevant shorter timescale is $T \sim (\alpha^2 D)^{-1}$, set by the time it takes the chemical to diffuse over the penetration depth. The appropriate scalings are then

$$x = \frac{1}{\alpha} \check{x} , \qquad t = \frac{1}{\alpha^2 D_{\mathrm{e}}} \check{t} , \qquad C = \frac{\alpha M_0}{A} \check{C} . \tag{35a–c}$$

The system becomes

$$\frac{\partial \check{C}}{\partial \check{t}} = \frac{\partial^2 \check{C}}{\partial \check{x}^2} - Da \, \mathrm{e}^{-\check{x}} \, \check{C} , \tag{36a}$$

subject to

$$\check{C} = 2\delta(\check{x}) \quad \text{at} \quad \check{t} = 0 , \qquad \frac{\partial \check{C}}{\partial \check{x}} = 0 \quad \text{at} \quad \check{x} = 0 , \qquad C \to 0 \quad \text{as} \quad \check{x} \to \infty \tag{36b–d}$$

So at leading order, we have a standard diffusion equation, with the similarity solution

$$\check{C}(\check{x}, \check{t}) = \frac{1}{\sqrt{\pi \check{t}}} \, e^{-\check{x}^2/(4\check{t})} . \tag{37}$$

Hence in this short initial period of time no mass is lost at leading order, and hence the initial condition on the outer solution $\tilde{C}$ for $t = O(\alpha^2 D_{\mathrm{e}}/(I_0 k)^2)$ is

$$\tilde{C} = 2\delta(\tilde{x}) \quad \text{at} \quad \tilde{t} = 0 . \tag{38}$$

Returning to dimensional variables, the leading-order problem for the outer region at larger times (34), (38) can be written as

$$\frac{\partial C}{\partial t} = D_{\mathrm{e}} \frac{\partial^2 C}{\partial x^2} , \tag{39a}$$

subject to

$$C = \frac{2M_0}{A} \delta(x) \quad \text{at} \quad t = 0 , \tag{39b}$$

$$D_{\mathrm{e}} \frac{\partial C}{\partial x} - I_0 k \, C = 0 \quad \text{at} \quad x = 0 , \qquad C \to 0 \quad \text{as} \quad x \to \infty . \tag{39c,d}$$

Despite the simple appearance of this PDE system, we believe that it can only be solved numerically. A numerical solution is shown in figure 9.

5.3　Model with water-content dependent diffusion

Having revisited in §5.1.4 the experimental data to allow us to fit a very simple model of the decay rate of chemical by photolysis we now consider how the model might be extended to account for the many other phenomena that might alter this behaviour in a field-based trial.

The first extension was to include an additional constant rate of degradation to account for microbial action on the chemical. This microbial rate is much smaller than the photolysis rate near the surface but acts throughout the soil depth. Many other additional physical phenomena might be included. However, the previous model indicated that photolysis only occurs in a very small layer near the surface of the soil and hence it would require only a very small effect to transport the chemical further into the depth of the soil. Moisture transport was seen as key to this transport and hence it was decided that the diffusion/dispersion phenomena may be dominant and so this was included. The previous discussion introduced such diffusion into the model and here we consider how this can best be incorporated to allow interpretation of field-data.

Conservation of mass of the chemical with concentration C, therefore requires that

$$\frac{\partial C}{\partial t} - \frac{\partial}{\partial x}\left(D_e \frac{\partial C}{\partial x}\right) = -k_p I_s e^{-\alpha x} C - k_m C. \tag{40}$$

where D_e is the constant diffusion/dispersion coefficient, k_m is the constant degradation rate due to microbes and both α and $k_p I_s$ are from the photolysis experiments. $k_m = 0.00866\text{days}^{-1}$ is calculated from a half-life of 80 days for microbial degradation. As we anticipate that all the interesting photolysis behaviour occurs in a narrow layer near the soil surface soil the model was only applied to a 2cm layer so that x goes between 0 and 2cm.

There was considerable discussion on the form of the diffusion/dispersion coefficient. It is well known that this diffusion coefficient depends on the soil's volumetric water content θ. It was decided that rather than attempting to model this diffusion coefficient from first principles we should exploit the models used in PEARL [4]. We note that 'Option 2' for the diffusion coefficient of a chemical in the liquid phase in the soil is $D_w \, 2.5 \, \theta^3$, where D_w is the diffusion coefficient of the chemical in water, after neglecting the effect of temperature on diffusion. For the calculations we used $D_w = 4.3 \times 10^{-1}\text{cm}^2/\text{day}$. This model is chosen principally because we have access to the parameters and variables it requires, although it is based on gas diffusion and may not be the best choice of model if more data such as the soil's porosity was available. In order to compare the model to the data from field trial the values of θ were taken from the PEARL output for the top level of the soil at 1.25cm.

Having discussed the diffusion of the chemical within a liquid phase we expect the diffusion of the chemical in the soil to be smaller due to the proportion of chemical bound to the soil and not free to diffuse. Hence we further modify the model and take

$$D_e = \frac{D_w \, 2.5 \, \theta^3}{1 + K} \tag{41}$$

where $K = 10$ is the partition coefficient for the chemical.

It is worth noting that an advection term, describing how water flowing through the soil transports the chemical, is omitted. This is primarily because of the difficulty in obtaining values for the water's velocity, which would vary both with time and soil depth depending on rainfall and evaporation processes, from the computational model. we anticipate that advection may not be negligible, but have not examined this aspect further.

To the model we imposed no-flux boundary conditions

$$\frac{\partial C}{\partial x} = 0 \quad \text{at} \quad x = 0, \tag{42}$$

$$\frac{\partial C}{\partial x} = 0 \quad \text{at} \quad x = 2\text{cm}, \tag{43}$$

at the top and bottom of the layer of soil.

A model is needed for the initial distribution of the chemical. Unlike the laboratory situation the chemical in the field-trial is applied by spraying and hence is concentrated in a very thin layer on the soil surface. For the purposes of the mathematical model it was assumed that this initial distribution was therefore a Delta function with

$$C = 2C_0 \delta(x) \quad \text{at} \quad t = 0, \tag{44}$$

where C_0 is the initial concentration of chemical applied and the factor 2 is the account for the fact that the chemical is applied at the surface.

This problem (40), (41), (43), and (44) was solved numerically in Matlab using the inbuilt function pdepe, which selects appropriate time stepping (see [3]). The code is included in appendix A. The comparison between these numerical results and the field data is shown in Figure 10.

The model is a reasonable fit for the data, especially considering its simplicity and the absence of free parameters in our model. There are however a number of parameters that have been chosen based on empirical data, that may not be known precisely. Further numerical experiments could be done to test the sensitivity of the results to these parameters and to the form of the diffusion coefficient.

6   Conclusions

From the investigation we have concluded the following ideas should be accounted for when considering the effect of photolysis in chemical degradation in field-trials. The variations of light intensity and shadowing can affect the rate of chemical decay by photolysis. In particular it appears this reduces the rate of decay of chemical below that to be expected from a flat surface. The very rough upper surface of the soil can not only affect the absorption of UV radiation but will also alter the distribution of the initial concentration of chemical on the surface and the evaporation of moisture from the surface. These variations are expected to be as important to the resulting degradation and transport of the chemical as the effect due to variations in illumination strength.
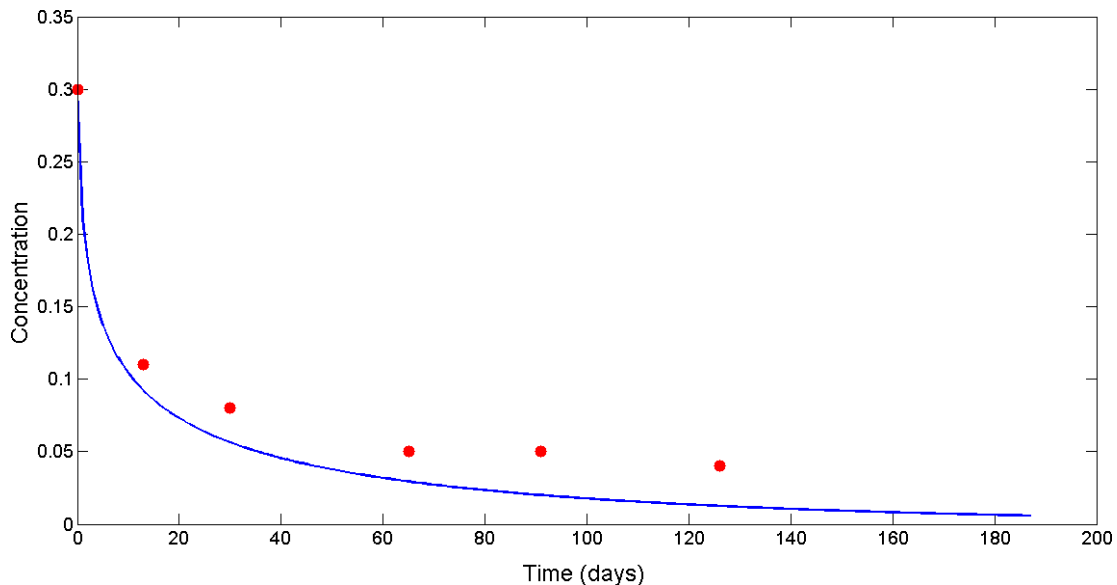
Figure 10: A comparison of field data from a Syngenta trial with the theoretical prediction from the model of §5.3. Non-dimensional concentration of chemical in the top 30cm of soil is plotted as a function of time.

When modelling the photolysis effect it is critical to account carefully for the decay of light intensity away from the surface. Our analysis here has presented a very simple model of this decay but, given the small decay distances and the size of the soil particles it may be very relevant to consider more carefully the electromagnetic problem of light incident on a rough particulate surface.

We have also seen that for a chemical that is initially distributed in a thin soil layer and is then acted upon by photolysis the resulting behaviour at the macroscopic level does not exhibit exponential decay. The high light intensity near the surface so causes the chemical to degrade very rapidly but deeper into the soil degradation is much slower, resulting in a longer tail. This non-exponential decay must be accounted for, in particular when interpreting data from laboratory experiments

Because of the very small distances that photolysis extends into the soil transport phenomena acting near the upper surface need to be considered very carefully. For the example considered here the water-dependent diffusion coefficient appears to be the critical parameter in predicting the observed behaviour. In other cases advection is anticipated to also be very important.

The current computational model of soil transport phenomena should be used with great care. The model has been developed for predicting large-scale behaviour and work well for such problems. The photolysis is have been show that accounting for behaviour on very small distances is critical and that accurate numerical methods may be required. It is not obvious that the current computational model can be exploited to give results in such cases.

References

[1] Bear, J., "Dynamics of fluids in porous media", Elvesier, New York, 1972.

[2] Bear J., "Hydraulics of groundwater flow", McGraw Hill, New York, 1979.

[3] MATLAB HELP GUIDE: pdepe (MATLAB Function Reference).

[4] ALTERRA REPORT, PEARL model for pesticide behaviour and emissions in soil-plant systems; Descriptions of the processes in FOCUS PEARL v 1.1.1. Alterra-rapport 013, ISSN 1566-7197. Link: http://www.pearl.pesticidemodels.eu/pdf/pearlthe.pdf

[5] Hebert V.R., Miller G.C., *Depth Dependence of Direct and Indirect Photolysis on Soil Surfaces*, J. Agric. Food Chem., **38**, pp913-918, 1990.

[6] Konstantinou I.K., Zarkadis A.K., Albanis T.A., *Photodegradation of Selected Herbicides in Various Natural Waters and Soils under Environmental Conditions*, J. Environ. Qual., **30**, pp121130 2001.

[7] Ciani A., Goss K.-U., Schwarzenbach R.P., *Light penetration in soil and particulate minerals* European Journal of Soil Science, **56**, pp561574, 2005.

[8] Frank M.P., Graebing P., Chib J.S., *Effect of Soil Moisture and Sample Depth on Pesticide Photolysis*, J. Agric. Food Chem., **50**, pp2607-2614, 2002.

[9] Fuentes C., Vauclin M., Parlange J-Y, Haverkamp R., *A Note on the Soil-Water Conductivity of a Fractal Soil*, Transport in Porous Media, **23**, pp31-36, 1996.

[10] Lehmann P, Stahli M., Papritz A., Gygi A., Fluher H., *A Fractal Approach to Model Soil Structure and to Calculate Thermal Conductivity of Soils*, Transport in Porous Media, **52**, pp313-332, 2003

[11] Richtmyer R.D., Morton K.W., "Difference Methods for Initial-Value Problems",Krieger, Florida, 1957.

[12] http://homepages.cwi.nl/ willem/Coll_AdvDiffReac/notes.pdf

A Matlab code for water-content diffusion model

The following code was used in MATLAB to solve the model in Section 5.3

```matlab
% Solve 1d diffusion problem using pdepe
function diffusion
global x u dx
m= 0;
Nt =188; %[T]=days
xend =2; %[L]=cm
Nx = 200;
x= linspace(0,xend,Nx);
dx=x(2)-x(1);
% Must be a sensible number of days
t= linspace(0,188-1,Nt);
pdexic2 = @(x) pdexic(x,dx);
sol= pdepe(m,@pdex,pdexic2,@pdexbc,x,t);
u= sol(:,:,1);
figure
surf(x,t,u); title(' pdepe soln');
shading interp
Cdepth=zeros(Nt,1);
for i=1:Nt
    Cdepth(i) = sum(u(i,2:end-1));
    Cdepth(i) = (Cdepth(i) + u(i,1)/2 + u(i,end)/2)*dx;
end
figure
plot(t,Cdepth)

function [c,f,s] = pdex(x,t,u,DuDx)
Nt=length(t);
load theta.mat
th = theta2(1:Nt);
De=4.3*2.5*10^(-2)*th.^3;
kp=2.28;
km=0.008664;
L=0.014;
c= 1;
f= De*DuDx;
s= -kp*exp(-x/L).*u - km*u;

function u0 = pdexic(x,dx)
u0 = 0.6/dx*(x==0);

function [pl,ql,pr,qr]= pdexbc(xl,ul,xr,ur,t)
pl= 0;
ql= 1;
pr= 0;
qr= 1;
```

The data for θ, the moisture content on the soil surface, as a function of time is given in the following table

t	θ	t	θ	t	θ	t	θ	t	θ	t	θ	t	θ
1	0.3984	29	0.3388	57	0.2861	85	0.2713	113	0.2640	141	0.3002	169	0.4483
2	0.4077	30	0.3352	58	0.2794	86	0.2708	114	0.2639	142	0.5153	170	0.4477
3	0.4014	31	0.3303	59	0.4959	87	0.2703	115	0.2651	143	0.5153	171	0.4478
4	0.3948	32	0.3251	60	0.3504	88	0.2699	116	0.5142	144	0.5127	172	0.4471
5	0.3974	33	0.3193	61	0.3100	89	0.2695	117	0.4184	145	0.5141	173	0.4465
6	0.3903	34	0.3139	62	0.3012	90	0.2691	118	0.3626	146	0.4806	174	0.4456
7	0.4877	35	0.3091	63	0.4759	91	0.2688	119	0.3489	147	0.5153	175	0.4449
8	0.4968	36	0.3753	64	0.3358	92	0.2684	120	0.3380	148	0.4779	176	0.4441
9	0.4483	37	0.3714	65	0.2931	93	0.2681	121	0.3269	149	0.4688	177	0.4439
10	0.4319	38	0.3568	66	0.2845	94	0.2678	122	0.3215	150	0.5144	178	0.4436
11	0.4188	39	0.3459	67	0.5134	95	0.2676	123	0.3135	151	0.5156	179	0.4434
12	0.4075	40	0.3441	68	0.3843	96	0.2673	124	0.3046	152	0.4794	180	0.4434
13	0.4016	41	0.3376	69	0.3575	97	0.2670	125	0.3015	153	0.4675	181	0.5123
14	0.3948	42	0.3338	70	0.3425	98	0.2668	126	0.3050	154	0.4624	182	0.5036
15	0.3959	43	0.3268	71	0.3342	99	0.2666	127	0.3809	155	0.5154	183	0.4864
16	0.4151	44	0.3218	72	0.3204	100	0.2663	128	0.4508	156	0.4845	184	0.4808
17	0.3979	45	0.3199	73	0.3155	101	0.2661	129	0.3981	157	0.5165	185	0.5150
18	0.3896	46	0.3160	74	0.3054	102	0.2659	130	0.3806	158	0.4817	186	0.4885
19	0.3826	47	0.3111	75	0.2960	103	0.2657	131	0.3627	159	0.5082	187	0.4887
20	0.3757	48	0.3115	76	0.2939	104	0.2655	132	0.3553	160	0.4852	188	0.4800
21	0.3675	49	0.3130	77	0.2882	105	0.2653	133	0.3416	161	0.4766		
22	0.3615	50	0.3159	78	0.2824	106	0.2651	134	0.3339	162	0.4675		
23	0.3630	51	0.5025	79	0.2772	107	0.2650	135	0.3261	163	0.4469		
24	0.3544	52	0.3988	80	0.2754	108	0.2648	136	0.3229	164	0.4417		
25	0.3508	53	0.3293	81	0.2743	109	0.2646	137	0.3198	165	0.4471		
26	0.3490	54	0.3062	82	0.2733	110	0.2645	138	0.3145	166	0.4499		
27	0.3426	55	0.2884	83	0.2726	111	0.2643	139	0.3102	167	0.4498		
28	0.3401	56	0.2957	84	0.2719	112	0.2642	140	0.3043	168	0.4495		

Table 1: Values of the water saturation θ in the top level of soil, recorded on each day t during over the course of a Syngenta field trial.

A Numerical diffusion/dispersion in advective diffusion problems

The problems associated with creating accurate and stable solutions to an advection diffusion equation representing the motion of a chemical within the soil is a very well studied problem. For further reading on this any standard text on numerical solution of partial differential equations will have a discussion on truncation errors and resulting numerical diffusion and dispersion. See for example the classic book [11].

In brief outline the behaviour can be seen by considering the simplest problem of advection with the equation

$$\frac{\partial C}{\partial t} + U\frac{\partial C}{\partial x} = 0 \tag{45}$$

where U is the velocity of the fluid transporting the chemical. Note the ideas readily extend to problems with diffusion and reactions.

One standard method for representing approximate numerical solutions to such problem is finite differences where C is considered to be evaluated at certain points (x_i, t_j) and the PDE is approximated by differences of these values. For example, assuming we know all the values of C up to time t_j then one common approximation is

$$\frac{C(x_i, t_{j+1}) - C(x_i, t_j)}{t_{j+1} - t_j} + U\frac{C(x_{i+1}, t_j) - C(x_{i-1}, t_j)}{x_{i+1} - x_{i-1}} = 0 \tag{46}$$

to calculate the values of $C(x_i, t_{j+1})$. This is called an explicit Euler timestep with spatial central differences. An alternative is to note that if $U > 0$ this implies that C is moving in the direction of increasing x. Hence, when calculating the next time values we should look for "where the C is coming from". This gives the approximation

$$\frac{C(x_i, t_{j+1}) - C(x_i, t_j)}{t_{j+1} - t_j} + U\frac{C(x_i, t_j) - C(x_{i-1}, t_j)}{x_{i-1} - x_i} = 0 \tag{47}$$

This is called an explicit Euler timestep with spatial upwind differences.

There are two issues to consider, firstly if the method is stable (is the answer sensitive to any small errors that may occur in the solution) and secondly is the method consistent (does it represent the PDE and if so how well). Analysis of these can be found and show the first is never stable while the second is if the timestep is sufficiently small (hence do not use the first approximation for this PDE although it may be adequate for diffusion problems). The accuracy can be indicated by using Taylor's theorem to approximate $C(x_i, t_{j+1})$ near (x_i, t_j). This gives

$$C(x_i, t_{j+1}) \approx C(x_i, t_j) + (t_{j+1} - t_j)\frac{\partial C}{\partial t}(x_i, t_j) + \frac{(t_{j+1} - t_j)^2}{2}\frac{\partial^2 C}{\partial t^2}(x_i, t_j) + \ldots \tag{48}$$

and similarly for $C(x_{i+1}, t_j)$ and so on.

From this we find that the central difference approximation gives the pde

$$\frac{\partial C}{\partial t} + U\frac{\partial C}{\partial x} + (t_{j+1} - t_j)\frac{\partial C}{\partial t} + \frac{U(x_{j+1} - x_j)^2}{6}\frac{\partial^3 C}{\partial x^3} + \ldots = 0 \tag{49}$$

while the upwind approximation gives

$$\frac{\partial C}{\partial t} + U\frac{\partial C}{\partial x} + (t_{j+1} - t_j)\frac{\partial C}{\partial t} + \frac{U(x_{j+1} - x_j)}{2}\frac{\partial^2 C}{\partial x^2} + \ldots = 0 \tag{50}$$

Now, if we want to get an accurate representation of the original PDE then in each case we need to take $(t_{j+1} - t_j)$ and $(x_{j+1} - x_j)$ very small (this is simply a statement that

small timesteps and fine grid spacings are needed for accuracy. However, we note that if we take small time steps, with $(t_{j+1} - t_j)$ small, but only use tolerably small space steps then the upwind method approximates a PDE with a diffusion coefficient of $U(x_{j+1} - x_j)/2$ while, the more accurate but unstable central difference scheme approximates a problem with no diffusion but dispersion, with coefficient $U(x_{j+1} - x_j)^2/6$. Hence we can consider that the use of particular numerical schemes on a problem that only has advection will produce numerical results that represent a problem where there is numerical diffusion or dispersion that depends on the approximation considered and the grid spacing used. In any reasonable code to solve an advection diffusion problem checks would be made to ensure that the solution found was insensitive to the grid spacing in order to avoid the solution being dominated by such behaviour rather than representing the true physical diffusion that is put into the equations. There are many advanced methods for solving such problems that greatly reduce these unwanted diffusive and dispersive effects (see for example [12].